Moroccan Journal of Chemistry
ISSN: 2351-812X
http://revues.imist.ma/?journal=morjchem&page=login
Ismail Warad / Mor. J. Chem. 9 N°1 (2021) 168-176

XRD/HSA-interactions, Hirshfeld analysis, HOMO/LUMO and MEP of new N'-(di(pyridin-2-yl)methylene DFT)benzohydrazide

Ismail Warad

Department of Chemistry and Earth Sciences, College of Arts and Sciences, Qatar University P. O. Box 2713, Doha, Qatar.

** Corresponding author:*
ismail.warad@qu.edu.qa

Received 03 Nov 2020,
Revised 23 Dec 2020,
Accepted 04 Jan 2021

Abstract

A new functionalized Schiff base N'-(di(pyridin-2-yl)methylene)benzohydrazide Schiff base (HZSB) was prepared in a high yield *via* condensation of benzohydrazide with di(pyridin-2-yl)methanone in ethanol solution under reflux condition. The prepared HZSB was characterized by XRD, DFT and computed *via* Hirshfeld surface analysis (HSA). The measured XRD structural parameters like angles lengths and bonds were matching with their DFT computed relatives.

Keywords: *Crystal structures; MEP; DFT, Hirshfeld surface.*

1. Introduction

Hydrazide Schiff base (HZSB) forms a wide variety of N,O-polychelate organic ligands, it can be prepared by condensation of hydrazide with aldehyde or ketone under reflux condition with and without using acid or base catalytic medium [1-6]. The imine –N=C together with carbonyl functional groups can promote such material to have pharmaceutical role in addition to being good bi-chelate N,O-ligands. HZSB are just motivating as they existing incorporation of donor centers, like a protonated/deprotonated C=N and O=C functional groups [1]. Therefore, such chelate with its bi-delocalization groups created several applications in clinical and biological fields like anti- anti-fungal, bacterial, anti-inflammatory, anti-convulsing, analgesic, anti-malarial, anti-tuberculosis, anti-cancer anti-platelets, and insecticidal [7-13]. These activities are assigned to the coordination ability of HZSB to form stable metal ions complexes that enhanced physiological procedures [14-16]. The coordination of HZSB with transition metal ions to form various complexes played a critical role in inorganic and organic applications [1-3]. Recently, several HZSB complexes with structural, biological chemical and industrial applications have been prepared [17-24]. Biological studies have reflected HZSB/complexes as significant DNA binding potential, as this interconnectedness may be an ambitious introduction to the development of therapeutic drugs for many diseases, especially cancer [17-19]. The preparation of HZSB has been performed *via* the condensation of benzohydrazide with di(pyridin-2-yl)methanone. The HZSB molecular structure was supported by the XRD-crystal and computed by DFT and HSA. The MEP, MAC, and NPA were served to support the XRD/HAS- interactions, moreover, DFT- bond lengths and angle values resembled to the XRD-measured parameters.

2. Materials and methods

2.1. Computational

Gaussian 09W 32 bit software was served for all DFT operations in gaseous state at DFT/B3LYP method and 6-311G(d) as basis set [25], the HSA and 2D-FP were carried out via Crystal Explorer 3.1 [26].

2.2. Chemicals

All chemicals and the solvents were purchased from Sigma-Aldrich and used without purification.

2.3. Synthesis of HZSB

Benzohydrazide (0.01 mol) was dissolved in 10 mL of ethanol, then added to stirring di(pyridin-2-yl)methanone (0.01 mol) dissolved 5 mL of ethanol. The reaction mixture was refluxed for 4 h, the precipitate product was filtrated and washed with *n*-hexane (81%, yield).

2.4. XRD-analysis

The structure was solved [24], with the SHELXT; the model was refined with version 2018/3 of SHELXL [27]. The crystal structure refinement parameters of the HZSB are illustrated in Table 1.

3. Results and Discussions

3.1. Synthesis, XRD and DFT

The N'-(di(pyridin-2-yl)methylene)benzohydrazide Schiff base (HZSB) product was prepared *via* one to one condensation of benzohydrazide with di(pyridin-2-yl)methanone in ethanol under reflux conditions for 4 hours, as seen in Scheme 1. Fig. 1 illustrates the XRD and DFT-structure analysis of the desired HZSB

ligand, which was crystallized in Monoclinic/$P2_1/c$, with the following lattice parameters: a = 8.2741(5), b =22.1436(14), and c = 8.8006(5) Å, meanwhile, β =108.974 (2)° [24]. The selected experimental XRD bond angle and bond lengths and the DFT outcome are illustrated in Table 2.

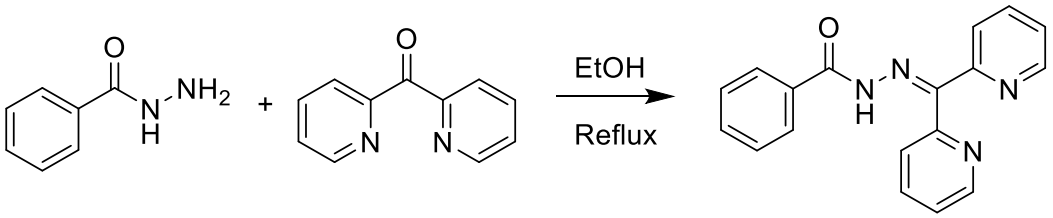

Scheme 1. Synthesis of desired HZSB ligand.

Table 1. Refined data of the HZSB

Chemical formula	$C_{18}H_{14}N_4O$
M_r	302.33
Crystal system, space group	Monoclinic, $P2_1/c$
Temperature (K)	295
a, b, c (Å)	8.2741 (5), 22.1436 (14), 8.8006 (5)
β (°)	108.974 (2)
V (Å^3)	1524.82 (15)
Z	4
Radiation type	Cu $K\alpha$
μ (mm^{-1})	0.09
Crystal size (mm)	0.50 × 0.30 × 0.10
Diffractometer	Rigaku R-AXIS RAPID
Absorption correction	Multi-scan (*SADABS*; Bruker, 2013)
T_{min}, T_{max}	0.968, 0.989
R_{int}	0.05
$(\sin \theta/\lambda)_{max}$ (Å^{-1})	0.64
$R[F^2 > 2\sigma(F^2)]$, $wR(F^2)$, S	0.053, 0.169, 0.99
$\Delta\rho_{max}$, $\Delta\rho_{min}$ (e Å^{-3})	0.15, −0.24

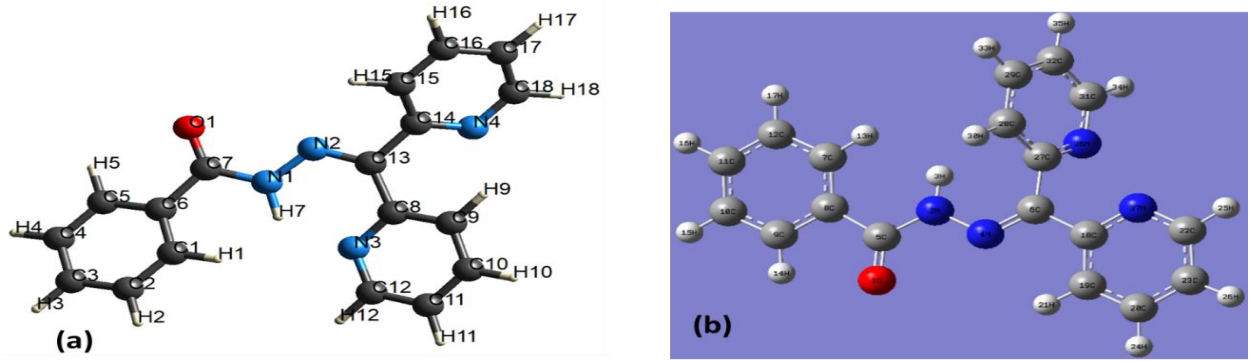

Fig.1. (a) Molecular structure and (b) DFT optimized of HZSB.

The angles and bond distance measured by XRD were matched to their relatives optimizes by DFT as seen in Fig. 2. A high level of coincidence between XRD and DFT was detected Fig. 2a. Graphical correlation of values of bond angles and bond lengths are given as R^2 = 0.992 and 0.995, respectively, Fig. 2b and Fig. 2d.

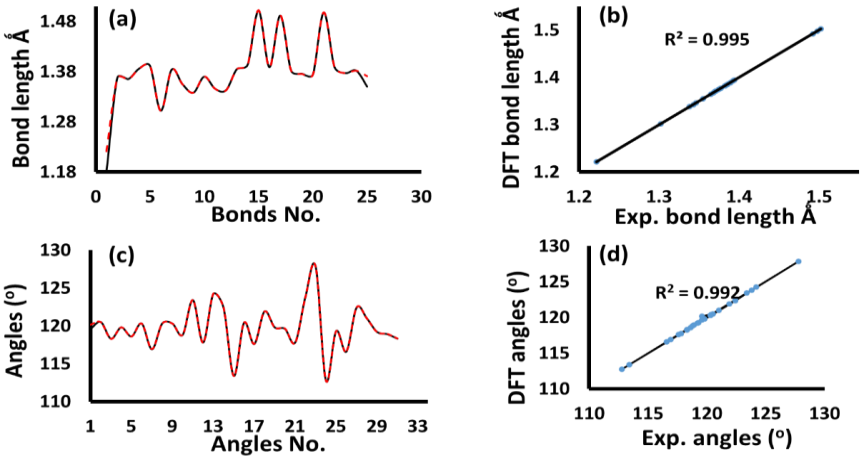

Fig. 2. (a) XRD/DFT-spectra of bond lengths, (c) DFT/XRD spectra of angles, (b) DFT/XRD-graphical correlation for bond lengths and (d) angles.

Table 2. Selected DFT/XRD-angles and bond distances.

Bond no.	Bond (Å)		XRD	DFT	Angles no.	Angles (°)			XRD	DFT
1	O1	C7	1.222(2)	1.2216	1	N2	N1	C7	120.2(1)	120.16
2	N1	N2	1.368(2)	1.3676	2	C2	C1	C6	120.5(2)	120.49
3	N1	C7	1.365(2)	1.3645	3	N1	N2	C13	118.3(1)	118.27
4	C1	C2	1.386(2)	1.3857	4	C1	C2	C3	119.8(2)	119.8
5	C1	C6	1.392(2)	1.3923	5	C8	N3	C12	118.6(1)	118.6
6	N2	C13	1.302(2)	1.3021	6	C2	C3	C4	120.3(2)	120.3
7	C2	C3	1.384(2)	1.3841	7	C14	N4	C18	116.9(2)	116.93
8	N3	C8	1.355(2)	1.355	8	C3	C4	C5	120.3(2)	120.29
9	N3	C12	1.338(2)	1.3382	9	C4	C5	C6	120.3(2)	120.3
10	C3	C4	1.370(2)	1.3705	10	C1	C6	C5	118.8(2)	118.81
11	N4	C14	1.346(2)	1.346	11	C1	C6	C7	123.4(1)	123.41
12	N4	C18	1.343(3)	1.3426	12	C5	C6	C7	117.8(1)	117.77
13	C4	C5	1.385(3)	1.3851	13	O1	C7	N1	124.2(2)	124.25
14	C5	C6	1.394(2)	1.3943	14	O1	C7	C6	122.4(2)	122.37
15	C6	C7	1.502(2)	1.5024	15	N1	C7	C6	113.4(1)	113.37
16	C8	C9	1.389(2)	1.3888	16	N3	C8	C9	120.4(1)	120.41
17	C8	C13	1.492(2)	1.4921	17	N3	C8	C13	117.6(1)	117.61
18	C9	C10	1.382(3)	1.3818	18	C9	C8	C13	121.9(1)	121.89
19	C10	C11	1.376(3)	1.3756	19	C8	C9	C10	119.8(2)	119.77
20	C11	C12	1.374(2)	1.3737	20	C9	C10	C11	119.6(2)	119.64
21	C13	C14	1.498(2)	1.4981	21	C10	C11	C12	117.8(2)	117.75
22	C14	C15	1.389(3)	1.3887	22	N3	C12	C11	123.8(2)	123.82
23	C15	C16	1.377(3)	1.3771	23	N2	C13	C8	127.8(1)	127.82
24	C16	C17	1.382(3)	1.382	24	N2	C13	C14	112.8(1)	112.78
25	C17	C18	1.371(4)	1.371	25	C8	C13	C14	119.3(1)	119.28

3.2. XRD/HAS-interactions

The connections in the crystal lattice of the desired HZSB have been determined *via* XRD-crystal as shown in Fig.3. Two types of hydrogen bonds were recorded, the first interaction was of type Ph-H….O=C with 2.618 Å, two bonds per molecule, as seen in Fig.3a, the second one was of type Ph-H….N-Py with 2.753 Å, also two bonds per molecule, as seen in Fig.3b.

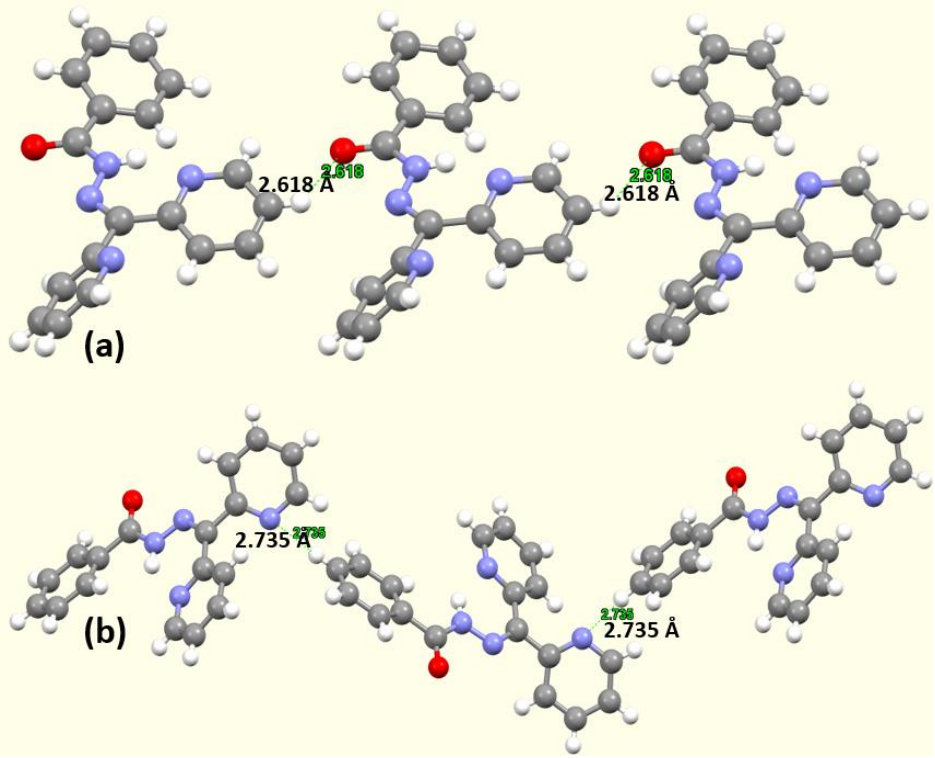

Fig. 3. All the interactions types. HZSB.

The HSA analysis was performed *via* CIF crystal data file of HZSB, as seen in Fig.4. The calculations [28-32] supported the formation of four red spots around the computed surface of the molecule which consistent with the formation of four H-bonds with types of H…N and H…O interactions as seen in d_{norm} (Fig.4a), no π-π phenyl stacks interactions of H…. π C=C bonds as shown in shape index (Fig.4b) and curvedness shapes (Fig.4c).

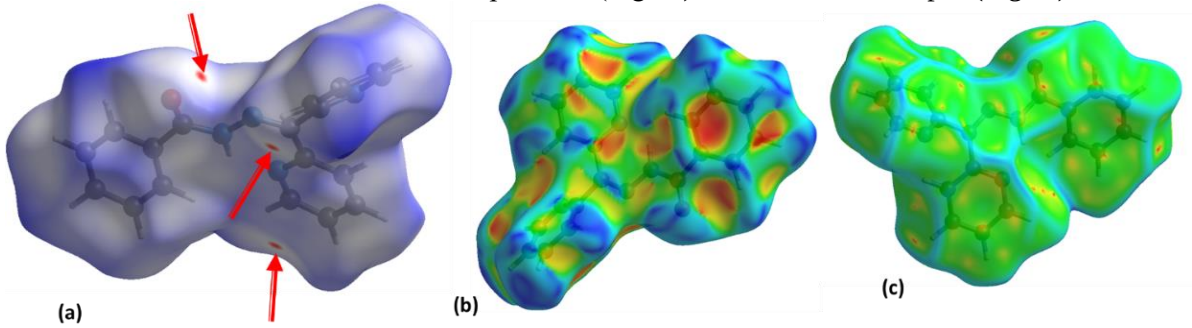

Fig. 4. (a) Mapped d_{norm}, (b) shape index, and (c) curvedness shapes.

3.3. 2D-FP

The fingerprint 2D-FP computational reflected the existence of different types of interactions with several H-to-atom contributions percentage, with the following order: H···H(42.5%)>C···H(11.7)>N···H(5.1%) >O···H(4.0%) as seen in Fig. 5a-d.

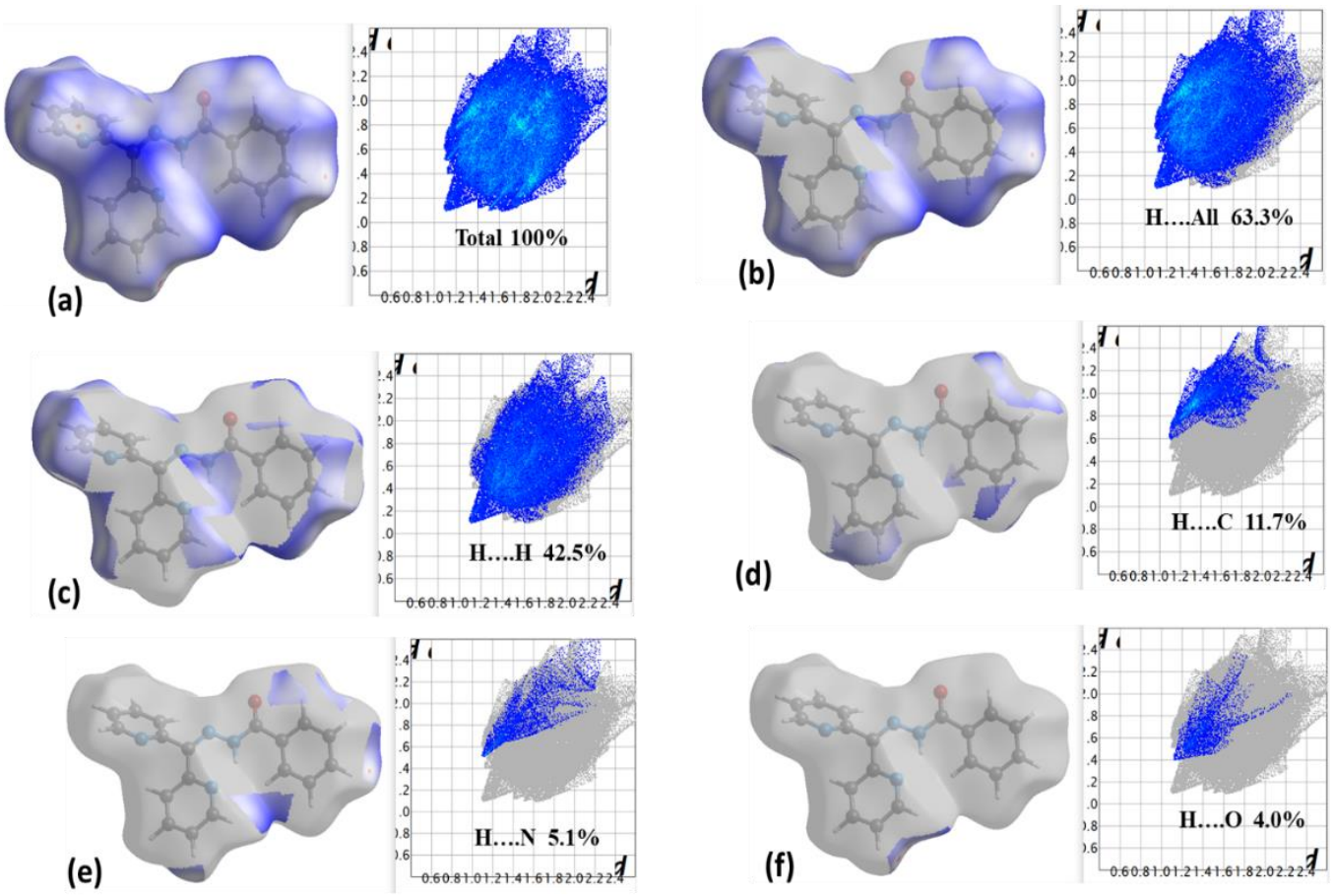

Fig. 5. 2D-FP H-to-atom contributions.

3.4. MEP, MAC and NPA

The MEP computation revealed the presence of blue (electrophilic) and red (nucleophilic) in addition to non-polarized (green) on the surface molecule [30-35]. The existence of four O and N atoms nucleophilic in their charge therefore, the red color was detected around these centers. The H of imide and same H's of the phenyl are poor in electron therefore; they appeared as blue in color (Fig.6a). The residue of the atoms centers are green due to electrophilic/nucleophilic properties. The existence of blue and red acceptors together in the surface raised up the possibility to form hydrogen bonds of types [H…..N] and [H….O]. The MAC and NPA charge destitution for each atoms is consistent with MEP result. Several e-rich/poor atoms were detected as seen in Table 3 and Fig.6b. In general, the NPA and MAC data are highly consistent with R^2 = 0.9188 as in Fig.5c. The NPA and MAC reflected all N, O and C atoms of with negative values, meantime, C in C=N, C in C=O and all the H's with positive charges. In the conclusion, the MEP, NPA and MAC result are harmonic with the XRD/HAS-interaction results.

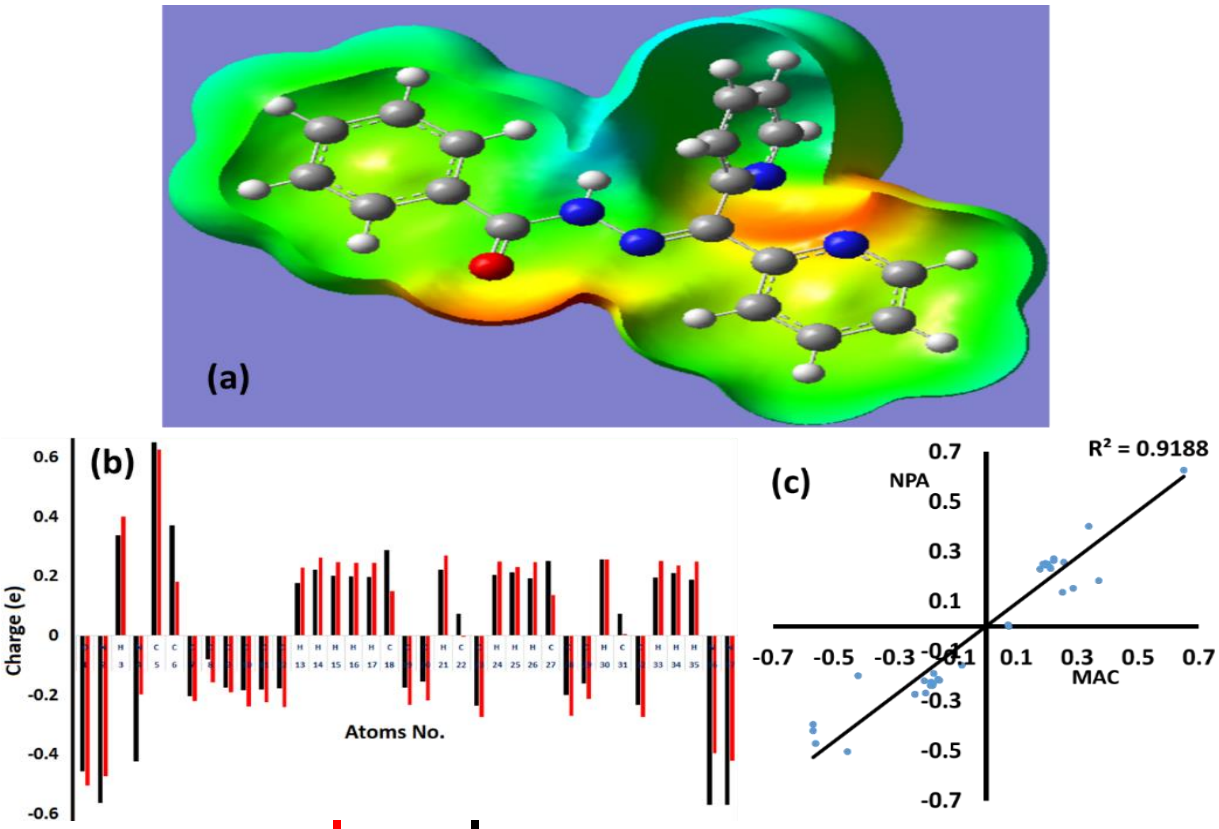

Fig.6. (a) MEP mapped: (b) NPA and MAC charges, and (c) NPA *vs*. MAC plot.

Table 3. NPA and MAC charges.

No.	Atom	MAC	NPA	No.	Atom	MAC	NPA
1	O	-0.45604	-0.50395	20	C	-0.15255	-0.21622
2	N	-0.56109	-0.47179	21	H	0.222041	0.27086
3	H	0.336623	0.40172	22	C	0.07395	-0.0003
4	N	-0.42037	-0.19759	23	C	-0.23312	-0.27351
5	C	0.649973	0.62623	24	H	0.202842	0.24984
6	C	0.369721	0.1825	25	H	0.211905	0.23127
7	C	-0.20343	-0.21946	26	H	0.191705	0.24667
8	C	-0.07853	-0.15575	27	C	0.250896	0.13701
9	C	-0.17279	-0.19036	28	C	-0.19893	-0.26888
10	C	-0.1812	-0.23812	29	C	-0.15847	-0.21332
11	C	-0.1794	-0.22342	30	H	0.256189	0.25782
12	C	-0.17624	-0.23916	31	C	0.073186	0.00538
13	H	0.177107	0.22969	32	C	-0.23278	-0.27304
14	H	0.222909	0.26434	33	H	0.195006	0.25197
15	H	0.20061	0.24738	34	H	0.21079	0.23606
16	H	0.198861	0.2454	35	H	0.188539	0.25041
17	H	0.196561	0.24522	36	N	-0.5681	-0.39507
18	C	0.286406	0.15181	37	N	-0.56874	-0.41985
19	C	-0.17406	-0.2318				

3.5. Molecular orbitals, DOS and Absorption/TD-DFT

The energy of electron transfer was determined by HOMO→LUMO and the density of state (DOS) methods as in Fig.7. The LUMO/HOMO FMO energy levels are both in negative area that increased the stability and softness of the HZSB. The $\Delta E_{HOMO/LUMO}$ was found to be with 4.490 eV (Fig.7a) whereas; the ΔE_{DOS} was with 4.510 eV (Fig.7b). Both methods used to calculate ΔE are very close in their values with 0.02 eV small deviation.

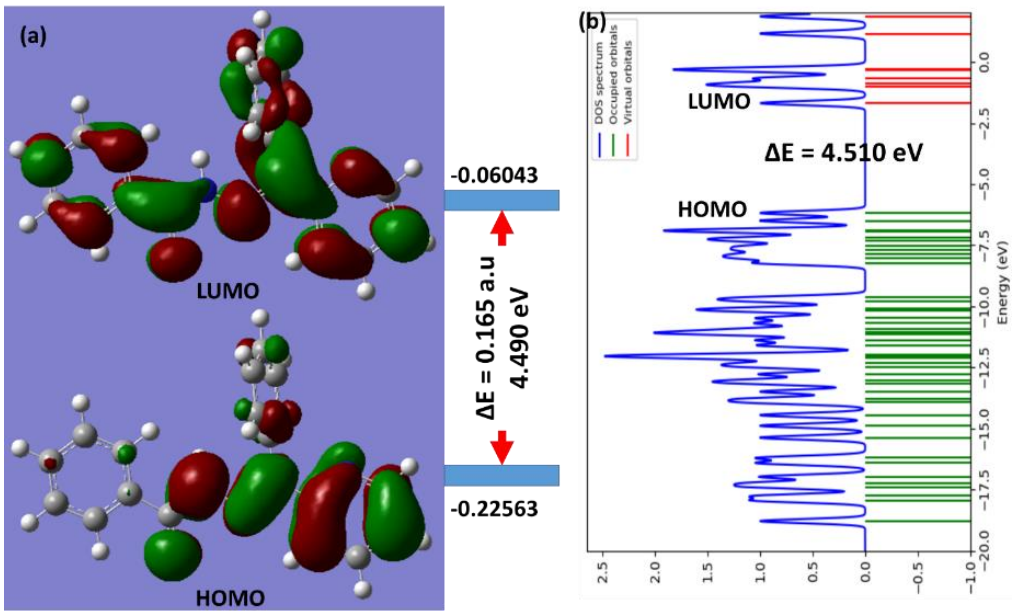

Fig.7. (a) LUMO/HOMO, and (b) DOS method for ΔE calculation.

4. Conclusions

The N'-(di(pyridin-2-yl)methylene)benzohydrazide Schiff base (HZSB) was made available in good yield *via* dehydration of di(pyridin-2-yl)methanone and benzohydrazide in ethanol under reflux condition. The XRD/HSA-interactions and DFT-optimization structure parameters matched well and confirmed the real 3D-structure of HZSB. Moreover, the MAC, NPA charge populations matched well with the MEP result.

References

[1] S. Mondal, B. Pakhira, A. J. Blake, M. Drew and S. K. Chattopadhyay. *Polyhedron* 117 (2016): 327–337

[2] I. Warad, A. A. Khan, M. Azam, S. I. Al-Resayes, and S. F. Haddad. *J. Mol. Struct.* 1062 (2014): 167-173.

[3] M. Azam, I. Warad, S. I. Al-Resayes, N. Alzaqri, M. R. Khan, R. Pallepogu, S. Dwivedi, J. Musarrat, and M. Shakir. *J. Mol. Struct.*, 1047 (2013): 48-54.

[4] V. Nagalakshmi, M. Sathya, M. Premkumar, D. Kaleeswaran, G. Venkatachalam, and K. Balasubramani, *J. Organomet. Chem.* 914 (2020): 121220-121230.

[5] I. Warad, M. Azam, U. Karama, S. Al-Resayes, A. Aouissi, and B. Hammouti. *J. Mol. Struct.*, 1002, (2011): 107-112.

[6] I. Warad, M. Abdoh, N. Shivalingegowda, N. K. Lokanath, R. Salghi, M. Al-Nuri, S. Radi, and B. Hammouti, *J. Mol. Struct.*,1099 (2015): 323-329.

[7] K.K. Bedia, O. Elçin, U. Seda, K. Fatma, S. Nathaly, R.A. Sevim, and A. Dimoglo, *Eur. J. Med. Chem.* 41 (2006) : 1253-1260.

[8] P. Melnyk, V. Leroux, C. Sergheraert, P. Grellier, and C. Sergheraert, *Bioorg. Med. Chem. Lett.* 16 (2006) 31-40.

[9] C. Cunha, J.M. Figueiredo, J.L.M. Tributino, A.L.P. Miranda, H.C. Castro, R.B. Zingali, C.A.M. Fraga, M.C.B. de Souza, V.F. Ferreira, and E. Barreiro, *J. Bioorg. Med. Chem*. 11 (2003): 2051-2061.
[10] L. Savanini, L. Chiasserini, A. Gaeta, and C. Pellerano, *Bioorg. Med. Chem.* 10 (2002): 2193-2199.
[11] R. Albertini, S. Pinelli, and P. Lunghi, *Inorg. Chim. Acta* 286 (1999) : 134-130.
[12] H. Elo, I. Sunila, and P. Lumme, *Inorg. Chim. Acta* 136 (1987) : 61-70.
[13] T. Todorovic, U. Rychlewska, B. Warzajtis, D. Radanovic, N. Filipovic, I. Pajic, D. Sladic, and K. Andelkovic, *Polyhedron* 28 (2009): 2397-2407.
[14] M. Katyal, and Y. Dutt, *Talanta* 22 (1975): 151-160.
[15] M. Mohan, M.P. Gupta, L. Chandra, and N.K. Jha, *Inorg. Chim. Acta* 151 (1988) : 61-70.
[16] S. A. Beyramabadi, M. Saadat-Far, A. Faraji-Shovey, M. Javan-Khoshkholgh, and A. Morsali, *J. Molec. Struc*., 1208 (2020): 127898-127905.
[17] Y. Liu, Na Wang, W. Mei, F. Chen, H. Li-Xin, L. Jian, and R. Wang, *Transition Met. Chem.* 32 (2007) : 332-340.
[18] I. Warad, A. A. F. Eftaiha, M. A. Al-Nuri, A. I. Husein, M. Assal, A. Abu-Obaid, N, Al-Zaqri, T. B. Hadda, and B. Hammouti. *J. Mater. Environ. Sci*., 4 (2013): 542-557.
[19] A. Mansri, B. Bouras, B. Hammouti, I. Warad, and A. Chetouani. *Res. Chem. Intermed.*, 39 (2013): 1753- 1765.
[20] M. Suleiman, M. Al-Masri, A. A. Ali, D. Aref, A. Hussein, I. Saadeddin, and I. Warad, *J Mater Environ Sci.* 6, (2015): 513-518.
[21] I. Warad, F. Eftaiha, M. Al-Nuri, I. Husein, M. Assal, A. Abu-Obaid, N. Al-Zaqri, B. Hadda and B. Hammouti, *J Mater Environ Sci.*, 4, (2013): 542-557.
[22] M. Rbaa, F. Benhiba, B. Obot, H. Oudda, I. Warad, B. Lakhrissi, and A. Zarrouk, *J. Molec. Liq.* 276 (2019): 120-133.
[23] S. Tighadouini, S. Radi, M. Bacquet, J.P. Dacquin, Y.N. Mabkhot, I.Warad, and M. Zaghrioui. *Sep. Sci. Technol.* 50 (2015): 710-717.
[24] I. Warad, M. Al-Nuri, S. Al-Resayes, K. Al-Farhana and M. Ghazzalia, *Acta Cryst*. E65 (2009) : 1597-1599.
[25] S. K. Wolff, D. J. Grimwood, J. J. McKinnon, D. Jayatilaka, and M. A. Spackman, Crystal explorer 2.1. University of Western Australia, Perth (2007).
[26] M.J. Frisch, G.W. Trucks, et. al. Gaussian 09, Gaussian Inc., Wallingford CT, 2009.
[27] G. M. Sheldrick, *Acta Cryst.*, A64 (2008): 112-114.
[28] I. Warad, M. R. H. Siddiqui, S. Al-Resayes, A. Al-Warthan, and R. Mahfouz, *Transit. Metal Chem*, 34, (2009): 347-352.
[29] I. Warad, Z. Al-Othman, S. Al-Resayes, S. S. Al-Deyab, and E. Kenawy. *Molecules* 15 (2010): 1028-1040. [30] M. E. Belghiti, Y. Karzazi, S. Tighadouini, A. Dafali, C. Jama, I. Warad, B. Hammouti, and S. Radi. *J Mater Environ Sci*., 7 (2016): 956-967.
[31] A. Chetouani, K. Medjahed, S. Al-Deyab, I. Warad, and A. Mansri, *J Mater Environ Sci.*, 7 (2012): 6025-6043.
[32] M. Belghiti, Y. Karzazi, S. Tighadouini, A. Dafal, C. Jama, I. Warad and B. Hammouti, and S. Radi, *J Mater Environ Sci.*, 7 (2016): 956-967.
[33] I. Warad, O. Bsharat, S. Tabti, A .Djedouani, M.Al-Nuri, N. Al-Zaqri, K. Kumara, N.K. Lokanath, S. Amereih, and Ib. M. Abu-Reidah, *J. Mol. Struct.*,1185 (2019): 290-299.
[34] M. R. Aouad, M. Messali, N. Rezki, N. Al-Zaqri, I. Warad, *J. Mol. Liq.*, 264 (2018): 621-630
[35] M. R. Aouad, M. Messali, N. Rezki, M. A. Said, D. Lentz, L. Zubaydi, I. Warad, *J. Mol. Struct.*,1180 (2019): 455-461.